

---

# Puppet-Master: Scaling Interactive Video Generation as a Motion Prior for Part-Level Dynamics

---

Ruining Li Chuanxia Zheng Christian Rupprecht Andrea Vedaldi  
Visual Geometry Group, University of Oxford  
{ruining, cxzheng, chrisr, vedaldi}@robots.ox.ac.uk

## Abstract

We present Puppet-Master, an interactive video generative model that can serve as a motion prior for *part-level* dynamics. At test time, given a single image and a sparse set of motion trajectories (*i.e.*, *drags*), Puppet-Master can synthesize a video depicting realistic part-level motion faithful to the given drag interactions. This is achieved by fine-tuning a large-scale pre-trained video diffusion model, for which we propose a new conditioning architecture to inject the dragging control effectively. More importantly, we introduce the *all-to-first* attention mechanism, a drop-in replacement for the widely adopted spatial attention modules, which significantly improves generation quality by addressing the appearance and background issues in existing models. Unlike other motion-conditioned video generators that are trained on in-the-wild videos and mostly move an entire object, Puppet-Master is learned from Objaverse-Animation-HQ, a new dataset of curated *part-level* motion clips. We propose a strategy to automatically filter out sub-optimal animations and augment the synthetic renderings with meaningful motion trajectories. Puppet-Master generalizes well to real images across various categories and outperforms existing methods in a *zero-shot* manner on a real-world benchmark. See our project page for more results: [vgg-puppetmaster.github.io](https://vgg-puppetmaster.github.io).

## 1 Introduction

We consider learning an open-ended model of the motion of natural objects, which can understand their *internal* dynamics. Most models of dynamic objects are ad-hoc and only work for a specific family of related objects, such as humans or quadrupeds [1, 2], severely limiting their generality. More open-ended models like [3] do not use such constrained shape priors but are difficult to scale due to the lack of suitable training data (*i.e.*, vertex-aligned 3D meshes). Therefore, we require a more general framework to learn a universal model of motion. This framework must be flexible enough to model very different types of internal dynamics (*e.g.*, part articulation, sliding of parts, and soft deformations). Furthermore, it must be able to tap substantial quantities of training data.

Recently, video generators learned from millions of videos have been proposed as proxies of world models, *i.e.*, models of any kind of natural phenomena, including motion. Such models may implicitly understand object dynamics; however, generating videos is insufficient: a useful model of object dynamics must be able to make *predictions* about the motion of given objects.

Inspired by DragAPart [4] and [5], we thus consider performing such predictions by learning a *conditional* video generator. This generator takes as input a single image of an object and one or more *drags* which specify the motion of selected physical points of the object; it then outputs a plausible video of the entire object motion consistent with the drags (Fig. 1).

Several authors have already considered incorporating drag-like motion prompts in image or video generation [6–18]. Many such works utilize techniques like ControlNet [19] to inject motion control in a pre-trained generator. However, these models tend to respond to drags by shifting or scaling an

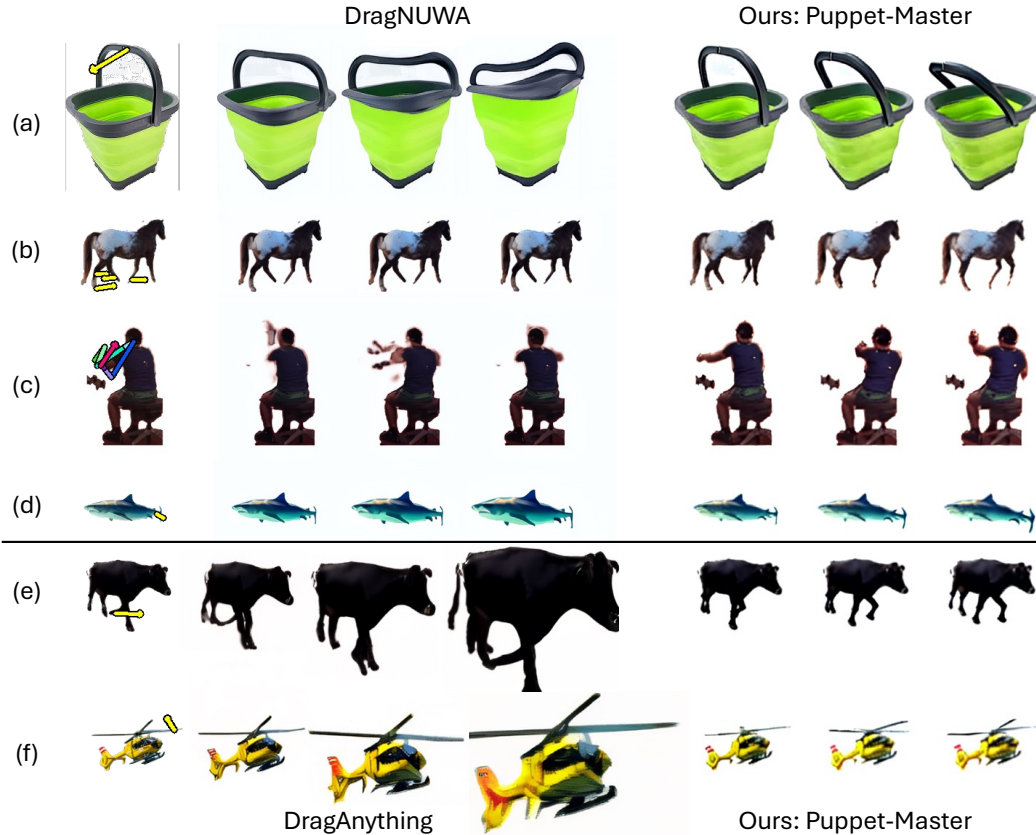


Figure 1: **Part-level dynamics vs. shifting or scaling an entire object.** Puppet-Master generates videos depicting *part-level* motion, prompted by one or more drags.

entire object and fail to capture their internal dynamics (Fig. 1), such as a drawer sliding out of a cabinet or a fish swinging its tail. The challenge is encouraging generative models to synthesize such internal, part-level dynamics.

While DragAPart has already considered this challenge, its results are limited for two reasons. First, the diversity of its training data is poor, as it primarily focuses on renderings of 3D furniture. Second, it starts from an image generator instead of a video generator. Consequently, it cannot benefit from the motion prior that a video generator trained on a large scale may already have captured, and can only capture the end frame of the motion.

In this work, we thus explore the benefits of learning a motion model from a pre-trained video generator while also significantly scaling the necessary training data to larger, more diverse sources. To do so, we start from Stable Video Diffusion (SVD) [20] and show how to re-purpose it for motion prediction. We make the following contributions.

First, we propose new conditioning modules to inject the dragging control into the video generation pipeline effectively. In particular, we find that *adaptive layer normalization* [21] is much more effective than the shift-based modulation proposed by [4]. We further observe that the cross-attention modules of the image-conditioned SVD model lack spatial awareness, and propose to add *drag tokens* to these modules for better conditioning. We also address the degradation in appearance quality that often arises when fine-tuning video generators on out-of-distribution datasets by introducing *all-to-first* attention, where all generated frames attend the first one via modified self-attention. This design creates a shortcut that allows information to propagate from the conditioning frame to the others directly, significantly improving generation quality.

Our second contribution is data curation: we provide two datasets to learn part-level object motion. Both datasets comprise subsets of the more than 40k animated assets from Objaverse [22]. These animations vary in quality: some display realistic object dynamics, while others feature objects

that (i) are static, (ii) exhibit simple translations, rotations, or scaling, or (iii) move in a physically implausible way. We introduce a systematic approach to curate the animations at scale. The resulting datasets, Objaverse-Animation and Objaverse-Animation-HQ, contain progressively fewer animations of higher quality. We show that Objaverse-Animation-HQ, which contains fewer but higher-quality animations, leads to a better model than Objaverse-Animation, demonstrating the effectiveness of the data curation.

With this, we train **Puppet-Master**, a video generative model that, given as input a single image of an object and corresponding drags, generates an animation of the object. These animations are *faithful to both the input image and the drags while containing physically plausible motions at the level of the individual object parts*. The same model works for a diverse set of object categories. Empirically, it outperforms prior works on multiple benchmarks. Notably, while our model is fine-tuned using only synthetic data, it generalizes well to real data, outperforming prior models that were fine-tuned on real videos. It does so in a *zero-shot* manner by generalizing to out-of-distribution, real-world data without further tuning.

## 2 Related Work

**Generative models.** Recent advances in generative models, largely powered by diffusion models [23–25], have enabled photo-realistic synthesis of images [26–28] and videos [29–31, 20], and been extended to various other modalities [32, 33]. The generation is mainly controlled by a text or image prompt. Recent works have explored ways to leverage these models’ prior knowledge, via either score distillation sampling [34–37] or fine-tuning on specialized data for downstream applications, such as multi-view images for 3D asset generation [38–43].

**Video generation for motion.** Attempts to model object motion often resort to pre-defined shape models, *e.g.*, SMPL [1] for humans and SMAL [2] for quadrupeds, which are constrained to a single or only a few categories. Videos have been considered as a unified representation that can capture general object dynamics [5]. However, existing video generators pre-trained on Internet videos often suffer from incoherent or minimal motion. Researchers have considered explicitly controlling video generation with motion trajectories. Drag-A-Video [44] extends the framework proposed by DragGAN [8] to videos. This method is training-free, relying on the motion prior captured by the pre-trained video generator, which is often not strong enough to produce high-quality videos. Hence, other works focus on training-based methods, which *learn* drag-based control using ad-hoc training data for this task. Early efforts such as iPoke [6] and YODA [45] train variational autoencoders or diffusion models to synthesize videos with objects in motion, conditioned on sparse motion trajectories sampled from optical flow. Generative Image Dynamics [10] uses a Fourier-based motion representation suitable for natural, oscillatory dynamics such as those of trees and candles, and generates motion for these categories with a diffusion model. DragNUWA [9] and others [11, 16–18] fine-tune pre-trained video generators on large-scale curated datasets, enabling drag-based control in open-domain video generation. However, these methods do *not* allow controlling motion at the level of object parts, as their training data entangles multiple factors, including camera viewpoint and object scaling and re-positioning, making it hard to obtain a model of part-level motion. Concurrent works leverage the motion prior captured by video generative models for the related 4D generation task [46–49]. These models, however, lack the capability of explicit dragging control, which we tackle in this work.

## 3 Method

Given a single image  $y$  of an object and one or more drags  $\mathcal{D} = \{d_k\}_{k=1}^K$ , our goal is to synthesize a video  $\mathcal{X} = \{x_i\}_{i=1}^N$  sampled from the distribution

$$\mathcal{X} \sim \mathbb{P}(x_1, x_2, \dots, x_N | y, \mathcal{D}) \quad (1)$$

where  $N$  is the number of video frames. The distribution  $\mathbb{P}$  should reflect physics and generate a *part-level* animation of the object that responds to the drags. To learn it, we capitalize on a pre-trained video generator, *i.e.*, Stable Video Diffusion (SVD, Section 3.1) [20]. Such video generators are expected to acquire an implicit, general-purpose understanding of motion through their pre-training

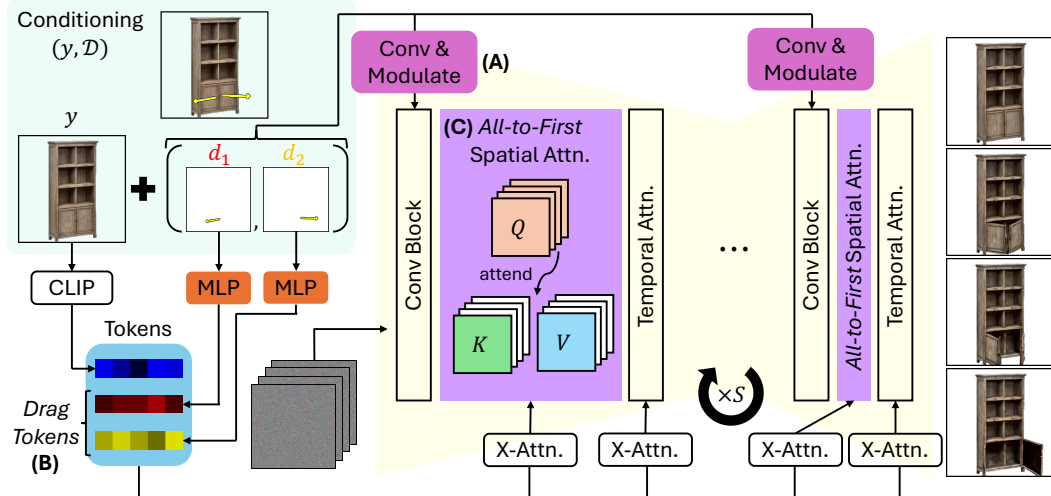


Figure 2: **Architectural Overview of Puppet-Master.** To enable precise drag conditioning, we first modify the original latent video diffusion architecture (Section 3.1) by (A) adding adaptive layer normalization modules to modulate the internal diffusion features and (B) adding cross attention with *drag tokens* (Section 3.2). Furthermore, to ensure high-quality appearance and background, we introduce (C) *all-to-first* spatial attention, a drop-in replacement for the spatial self-attention modules, which attends every noised video frame with the first frame (Section 3.3).

on Internet videos. This prior is particularly important to us, since we require data representative of *part-level* motions for our purposes, which are relatively scarce comparing to Internet videos.

In this section, we show how to tame the pre-trained video generator for part-level motion control. There are two main challenges. First, the drag conditioning must be injected into the video generation pipeline to facilitate efficient learning and accurate and time-consistent motion control while avoiding too much modifying the pre-trained video generator’s internal representation. Second, naively fine-tuning a pre-trained video diffusion model can result in artifacts such as cluttered backgrounds [39]. To address these challenges, in Section 3.2, we first introduce a novel mechanism to inject the drag condition  $\mathcal{D}$  in the video diffusion model. Then, in Section 3.3, we improve the video generation quality by introducing *all-to-first* attention mechanism, which reduces artifacts like the background clutter. Note that while we build on SVD, these techniques should be easily portable to other video generators based on diffusion.

### 3.1 Preliminaries: Stable Video Diffusion

SVD is an image-conditioned video generator based on diffusion, implementing a denoising process in latent space. This utilizes a variational autoencoder (VAE)  $(E, D)$ , where the encoder  $E$  maps the video frames to the latent space, and the decoder  $D$  reconstructs the video from the latent codes. During training, given a pair  $(\mathcal{X} = x^{1:N}, y)$  formed by a video and the corresponding image prompt, one first obtains the latent code as  $z_0^{1:N} = E(x^{1:N})$ , and then adds to the latter Gaussian noise  $\epsilon \sim \mathcal{N}(0, \mathbf{I})$ , obtaining the progressively more noised codes

$$z_t^{1:N} = \sqrt{\bar{\alpha}_t} z_0^{1:N} + \sqrt{1 - \bar{\alpha}_t} \epsilon^{1:N}, \quad t = 1, \dots, T. \quad (2)$$

This uses a pre-defined noising schedule  $\bar{\alpha}_0 = 1, \dots, \bar{\alpha}_T = 0$ . The denoising network  $\epsilon_\theta$  is trained to reverse this noising process by optimizing the objective function:

$$\min_{\theta} \mathbb{E}_{(x^{1:N}, y), t, \epsilon^{1:N} \sim \mathcal{N}(0, \mathbf{I})} [\|\epsilon^{1:N} - \epsilon_\theta(z_t^{1:N}, t, y)\|_2^2]. \quad (3)$$

Here,  $\epsilon_\theta$  uses the same U-Net architecture of VideoLDM [30], inserting temporal convolution and temporal attention modules after the spatial modules used in Stable Diffusion [27]. The image conditioning is achieved via (1) cross attention with the CLIP [50] embedding of the reference frame  $y$ ; and (2) concatenating the encoded reference image  $E(y)$  channel-wise to  $z_t^{1:N}$  as the input of the network. After  $\epsilon_\theta$  is trained, the model generates a video  $\hat{\mathcal{X}}$  prompted by  $y$  via iterative denoising from pure Gaussian noise  $z_T^{1:N} \sim \mathcal{N}(0, \mathbf{I})$ , followed by VAE decoding  $\hat{\mathcal{X}} = \hat{x}^{1:N} = D(z_0^{1:N})$ .

### 3.2 Adding Drag Control to Video Diffusion Models

Next, we show how to add the drags  $\mathcal{D}$  as an additional input to the denoiser  $\epsilon_\theta$  for motion control. We do so by introducing an encoding function for the drags  $\mathcal{D}$  and by extending the SVD architecture to inject the resulting code into the network. The model is then fine-tuned using videos combined with corresponding drag prompts in the form of training triplets  $(\mathcal{X}, y, \mathcal{D})$ . We summarize the key components of the model below and refer the reader to Appendix A for more details.

**Drag encoding.** Let  $\Omega$  be the spatial grid  $\{1, \dots, H\} \times \{1, \dots, W\}$  where  $H \times W$  is the resolution of a video. A drag  $d_k$  is a tuple  $(u_k, v_k^{1:N})$  specifying that the drag starts at location  $u_k \in \Omega$  in the reference image  $y$  and lands at locations  $v_k^n \in \Omega$  in subsequent frames. To encode a set of  $K \leq K_{\max} = 5$  drags  $\mathcal{D} = \{d_k\}_{k=1}^K$  we use the multi-resolution encoding of [4]. Each drag  $d_k^1$ , is input to a hand-crafted encoding function  $\text{enc}(\cdot, s) : \Omega^N \mapsto \mathbb{R}^{N \times s \times s \times c}$ , where  $s$  is the desired encoding resolution. The encoding function captures the state of the drag in each frame; specifically, each slice  $\text{enc}(d_k, s)[n]$  encodes (1) the drag’s starting location  $u_k$  in the reference image, (2) its intermediate location  $v_k^n$  in the  $n$ -th frame, and (3) its final location  $v_k^N$  in the final frame. The  $s \times s$  map  $\text{enc}(d_k, s)[n]$  is filled with values  $-1$  except in correspondence of the 3 locations, where we store  $u_k, v_k^n$  and  $v_k^N$  respectively, utilizing  $c = 6$  channels. Finally, we obtain the encoding  $\mathcal{D}_{\text{enc}}^s \in \mathbb{R}^{N \times s \times s \times c K_{\max}}$  of  $\mathcal{D}$  by concatenating the encodings of the  $K$  individual drags, filling extra channels with value  $-1$  if  $K < K_{\max}$ . The encoding function is further detailed in Appendix A.

**Drag modulation.** The SVD denoiser comprises a sequence of U-Net blocks operating at different resolutions  $s$ . We inject the drag encoding  $\mathcal{D}_{\text{enc}}^s$  in each block, matching the block’s resolution  $s$ . We do so via modulation using an adaptive normalization layer [21, 51–56]. Namely,

$$f_s \leftarrow f_s \otimes (\mathbf{1} + \gamma_s) + \beta_s, \quad (4)$$

where  $f_s \in \mathbb{R}^{B \times N \times s \times s \times C}$  is the U-Net features of resolution  $s$ , and  $\otimes$  denotes element-wise multiplication.  $\gamma_s, \beta_s \in \mathbb{R}^{B \times N \times s \times s \times C}$  are the *scale* and *shift* terms regressed from the drag encoding  $\mathcal{D}_{\text{enc}}^s$ . We use convolutional layers to embed  $\mathcal{D}_{\text{enc}}^s$  from the dimension  $cK_{\max}$  to the target dimension  $C$ . We empirically find that this mechanism provides better conditioning than using only a single shift term with *no* scaling as in [4].

**Drag tokens.** In addition to conditioning the network via drag modulation, we also do so via cross-attention by exploiting SVD’s cross-attention modules. These modules attend a *single* key-value obtained from the CLIP [50] encoding of the reference image  $y$ . Thus, they degenerate to a global bias term with *no* spatial awareness [57]. In contrast, we concatenate to the CLIP token additional *drag tokens* so that cross-attention is non-trivial. We use multi-layer perceptrons (MLPs) to regress an additional key-value pair from *each* drag  $d_k$ . The MLPs take the origin  $u_k$  and terminations  $v_k^n$  and  $v_k^N$  of  $d_k$  along with the internal diffusion features sampled at these locations, which are shown to contain semantic information [58], as inputs. Overall, the cross-attention modules have  $1 + K_{\max}$  key-value pairs (1 is the original image CLIP embedding), with extra pairs set to 0 if  $K < K_{\max}$ .

### 3.3 Attention with the Reference Image Comes to Rescue

In preliminary experiments utilizing the Drag-a-Move [4] dataset, we noted that the generated videos tend to have cluttered/gray backgrounds. Instant3D [39] reported a similar problem when generating multiple views of a 3D object, which they addressed via careful noise initialization. VideoMV [59] and Vivid-ZOO [60] directly constructed training videos with a gray background, which might help them offset a similar problem.

The culprit is that SVD, which was trained on  $576 \times 320$  videos, fails to generalize to very different resolutions. Indeed, when prompted by a  $256 \times 256$  image, SVD *cannot* generate reasonable videos. As a consequence, fine-tuning SVD on  $256 \times 256$  videos (as we do for Puppet-Master) is prone to local optima, yielding sub-optimal appearance details. Importantly, we noticed that the first frame of each generated video is spared from the appearance degradation (Fig. 6), as the model learns to directly copy the reference image. Inspired by this, we propose to create a “shortcut” from each noised frame to the first frame with *all-to-first* spatial attention, which significantly mitigates, if not completely resolves, the problem.

<sup>1</sup>With a slight abuse of notation, we assume  $d_k \in \Omega^N$ , as  $u_k = v_k^1$  and hence  $v_k^{1:N} \in \Omega^N$  fully describes  $d_k$ .

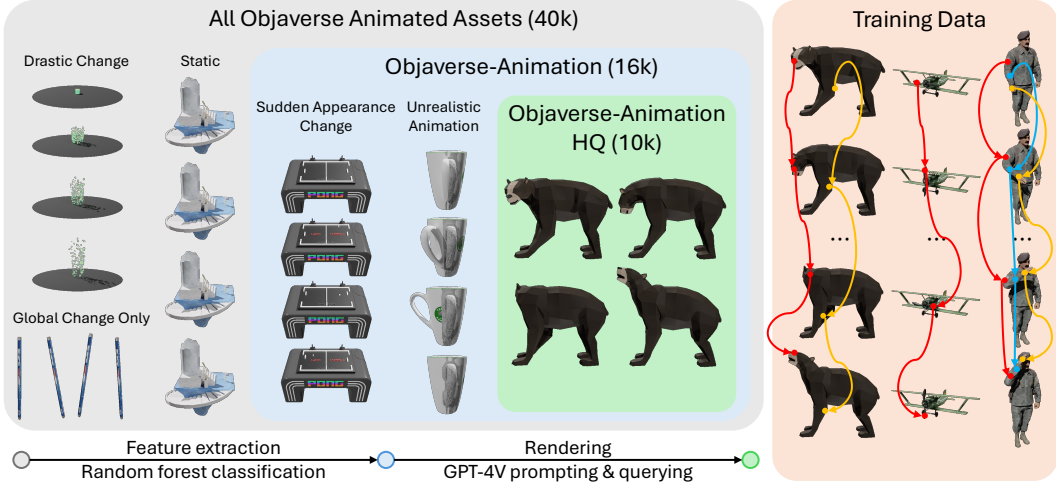


Figure 3: **Data Curation.** We propose two strategies to filter the animated assets in Objaverse, resulting in Objaverse-Animation (16k) and Objaverse-Animation-HQ (10k) of varying levels of curation, from which we construct the training data of Puppet-Master by sampling sparse motion trajectories and projecting them to 2D as drags.

**All-to-first spatial attention.** Previous works [61–63] have shown that attention between the noised branch and the reference branch improves the generation quality of image editing and novel view synthesis tasks. Here, we design an *all-to-first* spatial attention that enables each noised frame to attend to the first (reference) frame. Inspired by [63], we implement this attention by having each frame query the key and value of the first frame in all self-attention layers within the denoising U-Net. More specifically, denoting the query, key, and value tensors as  $Q, K$  and  $V \in \mathbb{R}^{B \times N \times s \times s \times C}$ , we discard the key and value tensors of non-first frames, *i.e.*,  $K[:, 1:]$  and  $V[:, 1:]$ , and compute the spatial attention  $A_i$  of the  $i$ -th frame as follows:

$$A_i = \text{softmax} \left( \frac{\text{flat}(Q[:, i]) \text{flat}(K[:, 0])^T}{\sqrt{D}} \right) \text{flat}(V[:, 0]), \quad (5)$$

where  $\text{flat}(\cdot) : \mathbb{R}^{B \times s \times s \times C} \mapsto \mathbb{R}^{B \times L \times C}$  flattens the spatial dimensions to get  $L = s \times s$  tokens for attention. The benefit is two-fold: first, this “shortcut” to the first frame allows each non-first frame to directly access non-degraded appearance details of the reference image, effectively alleviating local minima during optimization. Second, combined with the proposed drag encoding (Section 3.2), which specifies, for *every* frame, the origin  $u_k$  at the first frame, all-to-first attention enables the latent pixel containing the drag termination (*i.e.*,  $v_k^n$ ) to more easily attend to the latent pixel containing the drag origin on the first frame, potentially facilitating learning.

## 4 Curating Data to Learn Part-Level Object Motion

To train our model we require a video dataset that captures the motion of objects at the level of parts. Creating such a dataset in the real world means capturing a large number of videos of moving objects while controlling for camera and background motion. This is difficult to do for many categories (*e.g.*, animals) and unfeasible at scale. DragAPart [4] proposed to use instead renderings of synthetic 3D objects, and their corresponding part annotations, obtained from GPartNet [64]. Unfortunately, this dataset still requires to manually annotate and animate 3D object parts semi-manually, which limits its scale. We instead turn to Objaverse [22], a large-scale 3D dataset of 800k models created by 3D artists, among which about 40k are animated. In this section, we introduce a pipeline to extract suitable training videos from these animated 3D assets, together with corresponding drags  $\mathcal{D}$ .

**Identifying animations.** While Objaverse [22] has more than 40k assets labeled as animated, not all animations are useful for our purposes (Fig. 3). Notably, some are “fake”, with the objects remaining static throughout the sequence, while others feature drastic changes in the objects’ positions or even

their appearances. Therefore, our initial step is to filter out these unsuitable animations. To do so, we extract a sequence of aligned point clouds from each animated model and calculate several metrics for each sequence, including: (1) the dimensions and location of the bounding box encompassing the entire motion clip, (2) the size of the largest bounding box for the point cloud at any single timestamp and (3) the mean and maximal total displacement of all points throughout the sequence. Using these metrics, we fit a random forest classifier, which decides whether an animation should be included in the training videos or not, on a subset of Objaverse animations where the decision is manually labeled. The filtering excludes many assets that exhibit imperceptibly little or over-dramatic motions and results in a subset of 16k animations, which we dub Objaverse-Animation.

Further investigation reveals that this subset still contains assets whose motions are artificially conceived and therefore do not accurately mimic real-world dynamics (Fig. 3). To avoid such imaginary dynamics leaking into our synthesized videos, we employ the multi-modal understanding capability of GPT-4V [65] to assess the realism of each motion clip. Specifically, for each animated 3D asset in Objaverse-Animation, we fix the camera at the front view and render 4 images at timestamps corresponding to the 4 quarters of the animation and prompt GPT-4V to determine if the motion depicted is sufficiently realistic to qualify for the training videos. This filtering mechanism excludes another 6k animations, yielding a subset of 10k animations which we dub Objaverse-Animation-HQ.

**Sampling drags.** The goal of drag sampling is to produce a sparse set of drags  $\mathcal{D} = \{d_k\}_{k=1}^K$  where each drag  $d_k := (u_k, v_k^{1:N})$  tracks a point  $u_k$  on the asset in pixel coordinates throughout the  $N$  frames of rendered videos. To encourage the video generator to learn a meaningful motion prior, ideally, the set should be both *minimal* and *sufficient*: each group of independently moving parts should have *one* and *only one* drag corresponding to its motion trajectory, similar to Drag-a-Move [4]. For instance, there should be separate drags for different drawers of the same furniture, as their motions are independent, but not for a drawer and its handle, as in this case, the motion of one *implies* that of the other. However, Objaverse [22] lacks the part-level annotation to enforce this property. To partially overcome this, we find that some Objaverse assets are constructed in a bottom-up manner, consisting of multiple sub-models that align well with semantic parts. For these assets, we sample 1 drag per sub-model; for the rest, we sample a random number of drags in total. For each drag, we first sample a 3D point on the visible part of the model (or sub-model) with probabilities proportional to the point’s total displacement across  $N$  frames and then project its ground-truth motion trajectory  $p_1, \dots, p_N \in \mathbb{R}^3$  to pixel space to obtain  $d_k$ . Once all  $K$  drags are sampled, we apply a post-processing procedure to ensure that each pair of drags is sufficiently distinct, *i.e.*, for  $i \neq j$ , we randomly remove one of  $d_i$  and  $d_j$  if  $\|v_i^{1:N} - v_j^{1:N}\|_2^2 \leq \delta$  where  $\delta$  is a threshold we empirically set to  $20N$  for  $256 \times 256$  renderings.

## 5 Experiments

The final model, Puppet-Master, is trained on a combined dataset of Drag-a-Move [4] and Objaverse-Animation-HQ (Section 4). We evaluate the performance of the final checkpoint on multiple benchmarks, including the test split of Drag-a-Move and *real-world* cases from Human3.6M [66], Amazon-Berkeley Objects [67], Fauna Dataset [68, 69], and CC-licensed web images in a *zero-shot* manner, demonstrating qualitative and quantitative improvements over prior works and excellent generalization to real cases (Section 5.1). The design choices that led to Puppet-Master are ablated and discussed further in Section 5.2. In Section 5.3, we show the effectiveness of our data curation strategy (Section 4). We refer the reader to Appendix C for the implementation details.

### 5.1 Main Results

**Quantitative comparison.** We compare Puppet-Master to DragNUWA [9] and DragAnything [16], both of which are trained on real-world videos to support open-domain motion control, on the part-level motion-conditioned video synthesis task in Table 1. On the in-domain test set (*i.e.*, Drag-a-Move), Puppet-Master outperforms both methods on all standard metrics, including pixel-level PSNR, patch-level SSIM, and feature-level LPIPS and FVD, by a significant margin.

Additionally, to better demonstrate our model’s superiority in generating *part-level* object dynamics, we introduce a flow-based metric dubbed *flow error*. Specifically, we first track points on the object throughout the generated and ground-truth videos using CoTracker [70], and then compute flow error

Table 1: **Comparisons** with DragNUWA [9], DragAnything [16] and DragAPart [4] on the in-domain Drag-a-Move and out-of-domain Human3.6M datasets. The **best** method is bolded and second best underlined. Our model has *not* been trained on the Human3.6M dataset, or any real video datasets.

Method	Drag-a-Move [4]					Human3.6M [66]			
	PSNR↑	SSIM↑	LPIPS↓	FVD↓	flow error↓	PSNR↑	SSIM↑	LPIPS↓	FVD↓
DragNUWA	20.09	0.874	0.172	281.49	17.55 / 15.41	<u>17.52</u>	<b>0.878</b>	<u>0.158</u>	466.91
DragAnything	16.71	0.799	0.296	468.46	16.09 / 23.21	13.29	0.767	0.305	768.63
DragAPart									
— <i>Original</i>	23.41	0.925	0.085	180.27	14.17 / 3.71	15.14	0.852	0.197	683.40
— <i>Re-Trained</i>	<u>23.78</u>	<b>0.927</b>	<b>0.082</b>	<b>189.10</b>	<u>14.34 / 3.73</u>	15.25	0.860	0.188	549.64
Puppet-Master	<b>24.41</b>	<b>0.927</b>	<u>0.085</u>	<u>246.99</u>	<b>12.21 / 3.53</b>	<b>17.59</b>	<u>0.872</u>	<b>0.155</b>	<b>454.76</b>

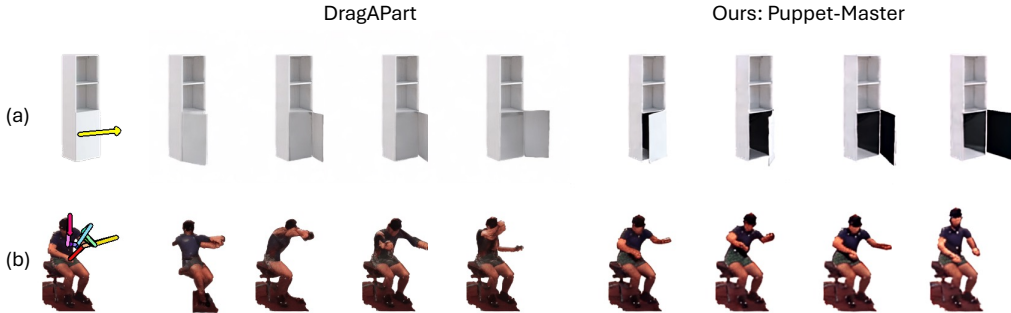


Figure 4: **Qualitative Comparison** with DragAPart [4]. The videos generated by DragAPart lack temporal consistency: (a) the door initially opens to the left, but later it is switched to open to the right, and it partially closes between the second and third frames visualized here; (b) DragAPart fails to generalize to out-of-domain cases, resulting in distorted motion.

as the root mean square error (RMSE) between the two trajectories. We report two RMSEs in Table 1 for this flow error metric. The former value (*i.e.*, before the slash) is averaged among the origins of all conditioning drags only, *i.e.*,  $\{u_k\}_{k=1}^K$ , while the latter value (*i.e.*, after the slash) is averaged among all foreground points. While Puppet-Master has lower values on both, it obtains a *significantly* smaller value when the error is averaged among all foreground points. This indicates Puppet-Master can better model nuanced *part-level* dynamics, thanks to which the parts that do not necessarily move along with the dragged parts stay static in the generated videos, reducing the overall error. By contrast, DragNUWA and DragAnything move the whole object, so every point incurs a large error.

To assess the cross-domain generalizability, we directly evaluate Puppet-Master on an unseen dataset captured in the real world (*i.e.*, Human3.6M). On this out-of-domain test set, Puppet-Master outperforms prior models on most metrics, despite not being fine-tuned on any real videos.

For completeness, we also include the metrics of DragAPart [4], a drag-conditioned image generator. The original DragAPart was trained on Drag-a-Move only. For fairness, we fine-tune it from Stable Diffusion [27] with the identical data setting as Puppet-Master, and evaluate the performance of both checkpoints (*Original*<sup>2</sup> and *Re-Trained* in Table 1). The videos are obtained from  $N$  independently generated frames conditioned on gradually extending drags. While its samples exhibit high visual quality in individual frames, they lack temporal smoothness, characterized by abrupt transitions and discontinuities in movement, resulting in a larger flow error<sup>3</sup> (Fig. 4a). This justifies starting from a video generator to improve temporal consistency. Furthermore, DragAPart fails to generalize to out-of-domain cases (*e.g.*, Fig. 4b and Table 1).

<sup>2</sup>*Original* is not ranked as it is trained on single-category data only and hence not an open-domain generator.

<sup>3</sup>FVD is not an informative metric for motion quality. Prior works [71, 72] have noted that FVD is biased towards the quality of individual frames and does *not* sufficiently account for motion in generated videos. Good FVD scores can still be obtained with static videos or videos with severe temporal corruption.





Figure 5: **Qualitative Results** on *real-world* cases spanning diverse categories.

**Qualitative comparison.** We show samples generated by Puppet-Master and prior models side by side in Fig. 1. The dynamics generated by Puppet-Master are physically plausible and faithful to the input image and drags. By contrast, the videos generated by DragNUWA [9] and DragAnything [16] scale (d, e, f) or shift (b) the object as a whole at best, or even show distorted motion (a, c). Even though Puppet-Master is fine-tuned solely on renderings of synthetic 3D models, it *does* generalize to real cases, and is capable of preserving fine-grained texture details.

**Qualitative results on real data.** In Fig. 5, we show more real examples generated by Puppet-Master. The synthesized videos exhibit realistic dynamics that are typical of the underlying categories, including humans, animals, and several man-made categories.

Table 2: **Ablation** studies of various model components. In addition to the standard metrics, we report a flow-based metric dubbed *flow error*. A lower flow error indicates the generated videos follow the drag control better. We also manually count the frequency of generated videos whose motion directions are opposite to the intention of their drag inputs. Here,  $\geq$  indicates there are video samples whose motion directions are hard to distinguish. When ablating attention with the reference image, we use  $\mathbb{C}$  as the base drag conditioning architecture.

Setting	PSNR $\uparrow$	SSIM $\uparrow$	LPIPS $\downarrow$	FVD $\downarrow$	flow error $\downarrow$	% wrong dir. $\downarrow$
<b>Drag conditioning</b>						
A Shift only w/o end loc.	13.23	0.816	0.446	975.16	15.60 px	$\geq 5$
B Shift+scale w/o end loc.	22.98	0.917	0.093	223.20	<b>9.33</b> px	4
C Shift+scale w/ end loc.	23.67	0.926	0.080	205.40	10.48 px	4
D $\mathbb{C}$ + x-attn. w/ drag tok.	<b>24.00</b>	<b>0.929</b>	<b>0.069</b>	<b>170.43</b>	9.80 px	<b>1</b>
<b>Attn. w/ ref. image</b>						
No attn.	11.96	0.771	0.391	823.00	12.35 px	$\geq 3$
Attn. w/ static ref. video	17.51	0.874	0.233	483.18	13.57 px	$\geq 8$
<i>All-to-first</i> attn.	<b>23.67</b>	<b>0.926</b>	<b>0.080</b>	<b>205.40</b>	<b>10.48</b> px	4

## 5.2 Ablations

We conduct several ablation studies to analyze the introduced components of Puppet-Master. For each design choice, we train a model using the training split of the Drag-a-Move [4] dataset with batch size 8 for 30,000 iterations and evaluate on 100 videos from its test split without classifier-free guidance [73]. Results are shown in Table 2 and Fig. 6 and discussed in detail next.

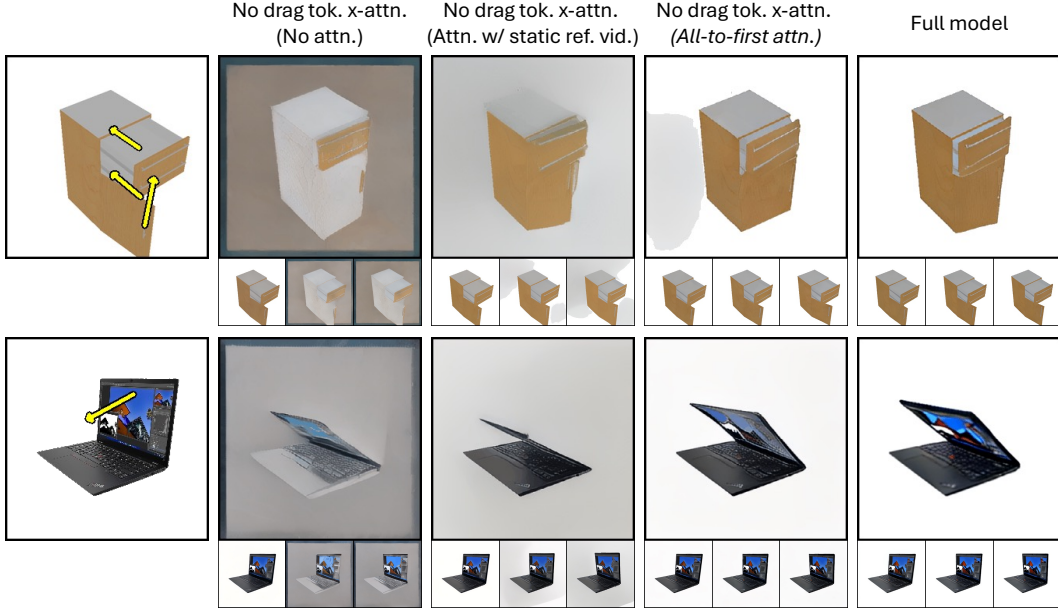


Figure 6: **Visualization** of samples generated by different model designs, where we show the last frame and the first 3 frames. While all designs produce nearly perfect first frames, our proposed *all-to-first* attention module significantly enhances sample quality. Without this module, the generated samples often exhibit sub-optimal appearances and backgrounds. The cross-attention module with drag tokens further improves the appearance details.

**Drag conditioning.** Table 2 compares Puppet-Master with multiple variants of conditioning mechanisms (Section 3.2). Adaptive normalization layers (A vs. B), drag encoding with final termination location  $v_k^N$  (B vs. C), and cross attention with drag tokens (C vs. D) are all beneficial. Notably, by combining these (*i.e.*, row D), the model achieves a negligible rate of generated samples with incorrect motion directions (see Table 2 caption for details).

**Attention with the reference image.** We find that *all-to-first attention* (Section 3.3) is essential for high generation quality. We also compare *all-to-first attention* with an alternative implementation strategy inspired by the X-UNet design in 3DiM [61], where we pass a static video consisting of the reference image copied  $N$  times to the same network architecture and implement cross attention between the clean (static) reference video branch and the noised video branch. The latter strategy performs worse. We hypothesize that this is due to the distribution drift between the two branches, which forces the optimization to modify the pre-trained SVD’s internal representations too much.

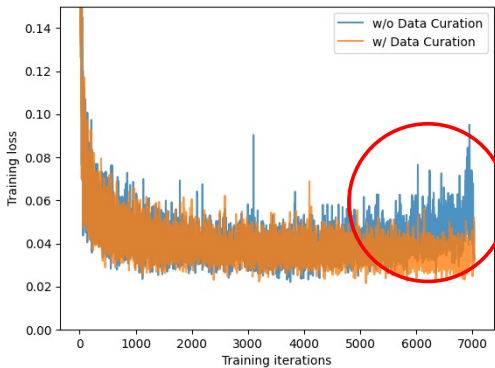


Figure 7: Data curation helps stabilize training.

Setting	PSNR $\uparrow$	SSIM $\uparrow$
w/o Data Curation	6.04	0.411
w/ Data Curation	<b>19.87</b>	<b>0.884</b>
Setting	LPIPS $\downarrow$	FVD $\downarrow$
w/o Data Curation	0.703	1475.35
w/ Data Curation	<b>0.181</b>	<b>624.47</b>

Table 3: Training on more abundant but lower-quality data leads to lower generation quality. Here, ‘w/o Data Curation’ model is trained on Objaverse-Animation while ‘w/ Data Curation’ model is trained on Objaverse-Animation-HQ. Both models are trained for 7K iterations. Evaluation is performed on the test split of Drag-a-Move [4].

### 5.3 Less is More: Data Curation Helps at Scale

To verify that our data curation strategy from Section 4 is effective, we compare two models trained on Objaverse-Animation and Objaverse-Animation-HQ respectively under the same hyper-parameter setting. The training dynamics are visualized in Fig. 7. The optimization collapses towards 7k iterations when the model is trained on a less curated dataset, resulting in much lower-quality video samples (Table 3). This suggests that the data’s quality matters more than quantity at scale.

## 6 Conclusion

We have introduced Puppet-Master, a model that can synthesize nuanced part-level motion in the form of a video, conditioned on sparse motion trajectories or drags. Fine-tuned from a large-scale pre-trained video generator on a carefully curated synthetic part-level motion dataset Objaverse-Animation-HQ, which we have contributed, our model demonstrates excellent *zero-shot* generalization to real-world cases. Thanks to the proposed adaptive layer normalization modules, the cross-attention modules with drag tokens and, perhaps more importantly, the all-to-first spatial attention modules, we have shown superior results compared to previous works on multiple benchmarks. Ablation studies verify the importance of the various components that contributed to this improvement.

**Acknowledgments.** This work is in part supported by a Toshiba Research Studentship, EPSRC SYN3D EP/Z001811/1, and ERC-CoG UNION 101001212. We thank Luke Melas-Kyriazi, Jinghao Zhou, Minghao Chen and Junyu Xie for useful discussions, Dejie Xu for sharing his experience developing CamCo [74], and RigManic, Inc. for providing the OpenAI credits essential for our research.

## References

- [1] Matthew Loper, Naureen Mahmood, Javier Romero, Gerard Pons-Moll, and Michael J. Black. SMPL: a skinned multi-person linear model. In *ACM TOG*, 2015.
- [2] Silvia Zuffi, Angjoo Kanazawa, David W. Jacobs, and Michael J. Black. 3D menagerie: Modeling the 3D shape and pose of animals. In *CVPR*, 2017.
- [3] Jiapeng Tang, Markhasin Lev, Wang Bi, Thies Justus, and Matthias Nießner. Neural shape deformation priors. In *NeurIPS*, 2022.
- [4] Ruining Li, Chuanxia Zheng, Christian Rupprecht, and Andrea Vedaldi. Dragapart: Learning a part-level motion prior for articulated objects. In *ECCV*, 2024.
- [5] Sherry Yang, Jacob Walker, Jack Parker-Holder, Yilun Du, Jake Bruce, Andre Barreto, Pieter Abbeel, and Dale Schuurmans. Video as the new language for real-world decision making. In *ICML*, 2024.
- [6] Andreas Blattmann, Timo Milbich, Michael Dorkenwald, and Björn Ommer. iPOKE: Poking a still image for controlled stochastic video synthesis. In *ICCV*, 2021.
- [7] Tsai-Shien Chen, Chieh Hubert Lin, Hung-Yu Tseng, Tsung-Yi Lin, and Ming-Hsuan Yang. Motion-conditioned diffusion model for controllable video synthesis. *arXiv preprint arXiv:2304.14404*, 2023.
- [8] Xingang Pan, Ayush Tewari, Thomas Leimkühler, Lingjie Liu, Abhimitra Meka, and Christian Theobalt. Drag your gan: Interactive point-based manipulation on the generative image manifold. In *ACM SIGGRAPH*, 2023.
- [9] Shengming Yin, Chenfei Wu, Jian Liang, Jie Shi, Houqiang Li, Gong Ming, and Nan Duan. Dragnuwa: Fine-grained control in video generation by integrating text, image, and trajectory. *arXiv preprint arXiv:2308.08089*, 2023.
- [10] Zhengqi Li, Richard Tucker, Noah Snavely, and Aleksander Holynski. Generative image dynamics. In *CVPR*, 2024.

- [11] Zhouxia Wang, Ziyang Yuan, Xintao Wang, Tianshui Chen, Menghan Xia, Ping Luo, and Ying Shan. Motionctrl: A unified and flexible motion controller for video generation. *arXiv preprint arXiv:2312.03641*, 2023.
- [12] Yujun Shi, Chuhui Xue, Jiachun Pan, Wenqing Zhang, Vincent YF Tan, and Song Bai. Dragdiffusion: Harnessing diffusion models for interactive point-based image editing. In *CVPR*, 2024.
- [13] Chong Mou, Xintao Wang, Jiechong Song, Ying Shan, and Jian Zhang. Dragondiffusion: Enabling drag-style manipulation on diffusion models. In *ICLR*, 2024.
- [14] Daniel Geng and Andrew Owens. Motion guidance: Diffusion-based image editing with differentiable motion estimators. In *ICLR*, 2024.
- [15] Pengyang Ling, Lin Chen, Pan Zhang, Huaian Chen, and Yi Jin. Freedrag: Point tracking is not you need for interactive point-based image editing. In *CVPR*, 2024.
- [16] Weijia Wu, Zhuang Li, Yuchao Gu, Rui Zhao, Yefei He, David Junhao Zhang, Mike Zheng Shou, Yan Li, Tingting Gao, and Di Zhang. Draganything: Motion control for anything using entity representation. In *ECCV*, 2024.
- [17] Chong Mou, Mingdeng Cao, Xintao Wang, Zhaoyang Zhang, Ying Shan, and Jian Zhang. Revideo: Remake a video with motion and content control. *arXiv preprint arXiv:2405.13865*, 2024.
- [18] Yaowei Li, Xintao Wang, Zhaoyang Zhang, Zhouxia Wang, Ziyang Yuan, Liangbin Xie, Yuexian Zou, and Ying Shan. Image conductor: Precision control for interactive video synthesis. *arXiv preprint arXiv:2406.15339*, 2024.
- [19] Lvmin Zhang, Anyi Rao, and Maneesh Agrawala. Adding conditional control to text-to-image diffusion models. In *ICCV*, 2023.
- [20] Andreas Blattmann, Tim Dockhorn, Sumith Kulal, Daniel Mendelevitch, Maciej Kilian, Dominik Lorenz, Yam Levi, Zion English, Vikram Voleti, Adam Letts, et al. Stable video diffusion: Scaling latent video diffusion models to large datasets. *arXiv preprint arXiv:2311.15127*, 2023.
- [21] Ethan Perez, Florian Strub, Harm De Vries, Vincent Dumoulin, and Aaron Courville. Film: Visual reasoning with a general conditioning layer. In *AAAI*, 2018.
- [22] Matt Deitke, Dustin Schwenk, Jordi Salvador, Luca Weihs, Oscar Michel, Eli VanderBilt, Ludwig Schmidt, Kiana Ehsani, Aniruddha Kembhavi, and Ali Farhadi. Objaverse: A universe of annotated 3d objects. In *CVPR*, 2023.
- [23] Jonathan Ho, Ajay Jain, and Pieter Abbeel. Denoising diffusion probabilistic models. In *NeurIPS*, 2020.
- [24] Yang Song and Stefano Ermon. Generative modeling by estimating gradients of the data distribution. In *NeurIPS*, 2019.
- [25] Yang Song, Jascha Sohl-Dickstein, Diederik P Kingma, Abhishek Kumar, Stefano Ermon, and Ben Poole. Score-based generative modeling through stochastic differential equations. In *ICLR*, 2021.
- [26] Aditya Ramesh, Mikhail Pavlov, Gabriel Goh, Scott Gray, Chelsea Voss, Alec Radford, Mark Chen, and Ilya Sutskever. Zero-shot text-to-image generation. In *ICML*, 2021.
- [27] Robin Rombach, Andreas Blattmann, Dominik Lorenz, Patrick Esser, and Björn Ommer. High-resolution image synthesis with latent diffusion models. In *CVPR*, 2022.
- [28] Chitwan Saharia, William Chan, Saurabh Saxena, Lala Li, Jay Whang, Emily L Denton, Kamyar Ghasemipour, Raphael Gontijo Lopes, Burcu Karagol Ayan, Tim Salimans, et al. Photorealistic text-to-image diffusion models with deep language understanding. In *NeurIPS*, 2022.

- [29] Jonathan Ho, William Chan, Chitwan Saharia, Jay Whang, Ruiqi Gao, Alexey Gritsenko, Diederik P Kingma, Ben Poole, Mohammad Norouzi, David J Fleet, et al. Imagen video: High definition video generation with diffusion models. *arXiv preprint arXiv:2210.02303*, 2022.
- [30] Andreas Blattmann, Robin Rombach, Huan Ling, Tim Dockhorn, Seung Wook Kim, Sanja Fidler, and Karsten Kreis. Align your latents: High-resolution video synthesis with latent diffusion models. In *CVPR*, 2023.
- [31] Rohit Girdhar, Mannat Singh, Andrew Brown, Quentin Duval, Samaneh Azadi, Sai Saketh Rambhatla, Akbar Shah, Xi Yin, Devi Parikh, and Ishan Misra. Emu video: Factorizing text-to-video generation by explicit image conditioning. *arXiv preprint arXiv:2311.10709*, 2023.
- [32] Guy Tevet, Sigal Raab, Brian Gordon, Yoni Shafir, Daniel Cohen-or, and Amit Haim Bermano. Human motion diffusion model. In *ICLR*, 2022.
- [33] Jiahui Lei, Congyue Deng, Bokui Shen, Leonidas Guibas, and Kostas Daniilidis. Nap: Neural 3d articulation prior. In *NeurIPS*, 2023.
- [34] Ben Poole, Ajay Jain, Jonathan T. Barron, and Ben Mildenhall. DreamFusion: Text-to-3d using 2d diffusion. In *ICLR*, 2023.
- [35] Chen-Hsuan Lin, Jun Gao, Luming Tang, Towaki Takikawa, Xiaohui Zeng, Xun Huang, Karsten Kreis, Sanja Fidler, Ming-Yu Liu, and Tsung-Yi Lin. Magic3d: High-resolution text-to-3d content creation. In *CVPR*, 2023.
- [36] Luke Melas-Kyriazi, Iro Laina, Christian Rupprecht, and Andrea Vedaldi. Realfusion: 360deg reconstruction of any object from a single image. In *Proceedings of the IEEE/CVF conference on computer vision and pattern recognition (CVPR)*, pages 8446–8455, 2023.
- [37] Tomas Jakab, Ruining Li, Shangzhe Wu, Christian Rupprecht, and Andrea Vedaldi. Farm3D: Learning articulated 3d animals by distilling 2d diffusion. In *3DV*, 2024.
- [38] Ruoshi Liu, Rundi Wu, Basile Van Hoorick, Pavel Tokmakov, Sergey Zakharov, and Carl Vondrick. Zero-1-to-3: Zero-shot one image to 3d object. In *ICCV*, 2023.
- [39] Jiahao Li, Hao Tan, Kai Zhang, Zexiang Xu, Fujun Luan, Yinghao Xu, Yicong Hong, Kalyan Sunkavalli, Greg Shakhnarovich, and Sai Bi. Instant3D: Fast text-to-3D with sparse-view generation and large reconstruction model. In *ICLR*, 2024.
- [40] Luke Melas-Kyriazi, Iro Laina, Christian Rupprecht, Natalia Neverova, Andrea Vedaldi, Oran Gafni, and Filippos Kokkinos. Im-3d: Iterative multiview diffusion and reconstruction for high-quality 3d generation. In *ICLR*, 2024.
- [41] Chuanxia Zheng and Andrea Vedaldi. Free3d: Consistent novel view synthesis without 3d representation. In *CVPR*, 2024.
- [42] Vikram Voleti, Chun-Han Yao, Mark Boss, Adam Letts, David Pankratz, Dmitry Tochilkin, Christian Laforte, Robin Rombach, and Varun Jampani. Sv3d: Novel multi-view synthesis and 3d generation from a single image using latent video diffusion. *arXiv preprint arXiv:2403.12008*, 2024.
- [43] Ruiqi Gao, Aleksander Holynski, Philipp Henzler, Arthur Brussee, Ricardo Martin-Brualla, Pratul Srinivasan, Jonathan T Barron, and Ben Poole. Cat3d: Create anything in 3d with multi-view diffusion models. *arXiv preprint arXiv:2405.10314*, 2024.
- [44] Yao Teng, Enze Xie, Yue Wu, Haoyu Han, Zhenguo Li, and Xihui Liu. Drag-a-video: Non-rigid video editing with point-based interaction. *arXiv preprint arXiv:2312.02936*, 2023.
- [45] Aram Davtyan and Paolo Favaro. Learn the force we can: Enabling sparse motion control in multi-object video generation. In *AAAI*, 2024.
- [46] Hanwen Liang, Yuyang Yin, Dejjia Xu, Hanxue Liang, Zhangyang Wang, Konstantinos N Plataniotis, Yao Zhao, and Yunchao Wei. Diffusion4d: Fast spatial-temporal consistent 4d generation via video diffusion models. *arXiv preprint arXiv:2405.16645*, 2024.

- [47] Haiyu Zhang, Xinyuan Chen, Yaohui Wang, Xihui Liu, Yunhong Wang, and Yu Qiao. 4diffusion: Multi-view video diffusion model for 4d generation. *arXiv preprint arXiv:2405.20674*, 2024.
- [48] Yanqin Jiang, Chaohui Yu, Chenjie Cao, Fan Wang, Weiming Hu, and Jin Gao. Animate3d: Animating any 3d model with multi-view video diffusion. *arXiv preprint arXiv:2407.11398*, 2024.
- [49] Yiming Xie, Chun-Han Yao, Vikram Voleti, Huaizu Jiang, and Varun Jampani. SV4D: Dynamic 3d content generation with multi-frame and multi-view consistency. *arXiv preprint arXiv:2407.17470*, 2024.
- [50] Alec Radford, Jong Wook Kim, Chris Hallacy, Aditya Ramesh, Gabriel Goh, Sandhini Agarwal, Girish Sastry, Amanda Askell, Pamela Mishkin, Jack Clark, et al. Learning transferable visual models from natural language supervision. In *ICML*, 2021.
- [51] Vincent Dumoulin, Jonathon Shlens, and Manjunath Kudlur. A learned representation for artistic style. In *ICLR*, 2016.
- [52] Tero Karras, Samuli Laine, and Timo Aila. A style-based generator architecture for generative adversarial networks. In *CVPR*, 2019.
- [53] Prafulla Dhariwal and Alexander Quinn Nichol. Diffusion models beat GANs on image synthesis. In *NeurIPS*, 2021.
- [54] Chuanxia Zheng, Tung-Long Vuong, Jianfei Cai, and Dinh Phung. Movq: Modulating quantized vectors for high-fidelity image generation. In *NeurIPS*, 2022.
- [55] William Peebles and Saining Xie. Scalable diffusion models with transformers. In *ICCV*, 2023.
- [56] Nanye Ma, Mark Goldstein, Michael S Albergo, Nicholas M Boffi, Eric Vanden-Eijnden, and Saining Xie. Sit: Exploring flow and diffusion-based generative models with scalable interpolant transformers. In *ECCV*, 2024.
- [57] Ido Sobol, Chenfeng Xu, and Or Litany. Zero-to-hero: Enhancing zero-shot novel view synthesis via attention map filtering. *arXiv preprint arXiv:2405.18677*, 2024.
- [58] Dmitry Baranchuk, Andrey Voynov, Ivan Rubachev, Valentin Khulkov, and Artem Babenko. Label-efficient semantic segmentation with diffusion models. In *ICLR*, 2021.
- [59] Qi Zuo, Xiaodong Gu, Lingteng Qiu, Yuan Dong, Zhengyi Zhao, Weihao Yuan, Rui Peng, Siyu Zhu, Zilong Dong, Liefeng Bo, et al. Videomv: Consistent multi-view generation based on large video generative model. *arXiv preprint arXiv:2403.12010*, 2024.
- [60] Bing Li, Cheng Zheng, Wenxuan Zhu, Jinjie Mai, Biao Zhang, Peterm Wonka, and Bernard Ghanem. Vivid-zoo: Multi-view video generation with diffusion model. *arXiv preprint arXiv:2406.08659*, 2024.
- [61] Daniel Watson, William Chan, Ricardo Martin Brualla, Jonathan Ho, Andrea Tagliasacchi, and Mohammad Norouzi. Novel view synthesis with diffusion models. In *ICLR*, 2023.
- [62] Mingdeng Cao, Xintao Wang, Zhongang Qi, Ying Shan, Xiaohu Qie, and Yinqiang Zheng. Masactrl: Tuning-free mutual self-attention control for consistent image synthesis and editing. In *ICCV*, 2023.
- [63] Haohan Weng, Tianyu Yang, Jianan Wang, Yu Li, Tong Zhang, CL Chen, and Lei Zhang. Consistent123: Improve consistency for one image to 3d object synthesis. *arXiv preprint arXiv:2310.08092*, 2023.
- [64] Haoran Geng, Helin Xu, Chengyang Zhao, Chao Xu, Li Yi, Siyuan Huang, and He Wang. Gapartnet: Cross-category domain-generalizable object perception and manipulation via generalizable and actionable parts. In *CVPR*, 2023.
- [65] OpenAI. Gpt-4 technical report. *arXiv preprint arXiv:2303.08774*, 2023.

- [66] Catalin Ionescu, Dragos Papava, Vlad Olaru, and Cristian Sminchisescu. Human3.6m: Large scale datasets and predictive methods for 3d human sensing in natural environments. *PAMI*, 2014.
- [67] Jasmine Collins, Shubham Goel, Kenan Deng, Achleshwar Luthra, Leon Xu, Erhan Gundogdu, Xi Zhang, Tomas F Yago Vicente, Thomas Dideriksen, Himanshu Arora, Matthieu Guillaumin, and Jitendra Malik. Abo: Dataset and benchmarks for real-world 3d object understanding. In *CVPR*, 2022.
- [68] Shangzhe Wu, Ruining Li, Tomas Jakab, Christian Rupprecht, and Andrea Vedaldi. Magicpony: Learning articulated 3d animals in the wild. In *CVPR*, 2023.
- [69] Zizhang Li, Dor Litvak, Ruining Li, Yunzhi Zhang, Tomas Jakab, Christian Rupprecht, Shangzhe Wu, Andrea Vedaldi, and Jiajun Wu. Learning the 3d fauna of the web. In *CVPR*, 2024.
- [70] Nikita Karaev, Ignacio Rocco, Benjamin Graham, Natalia Neverova, Andrea Vedaldi, and Christian Rupprecht. Cotracker: It is better to track together. In *ECCV*, 2024.
- [71] Songwei Ge, Aniruddha Mahapatra, Gaurav Parmar, Jun-Yan Zhu, and Jia-Bin Huang. On the content bias in fréchet video distance. In *CVPR*, 2024.
- [72] Daniel Watson, Saurabh Saxena, Lala Li, Andrea Tagliasacchi, and David J Fleet. Controlling space and time with diffusion models. *arXiv preprint arXiv:2407.07860*, 2024.
- [73] Jonathan Ho and Tim Salimans. Classifier-free diffusion guidance. *arXiv preprint arXiv:2207.12598*, 2022.
- [74] Dejia Xu, Weili Nie, Chao Liu, Sifei Liu, Jan Kautz, Zhangyang Wang, and Arash Vahdat. Camco: Camera-controllable 3d-consistent image-to-video generation. *arXiv preprint arXiv:2406.02509*, 2024.
- [75] Lingteng Qiu, Guanying Chen, Xiaodong Gu, Qi Zuo, Mutian Xu, Yushuang Wu, Weihao Yuan, Zilong Dong, Liefeng Bo, and Xiaoguang Han. Richdreamer: A generalizable normal-depth diffusion model for detail richness in text-to-3d. In *CVPR*, 2024.

## A Additional Details of the Drag Encoding

Here, we give a formal definition of  $\text{enc}(\cdot, s)$  introduced in Section 3.2. Recall that  $\text{enc}(\cdot, s)$  encodes each drag  $d_k := (u_k, v_k^{1:N})$  into an embedding of shape  $N \times s \times s \times 6$ . For each frame  $n$ , the first, middle, and last two channels (of the  $c = 6$  in total) encode the spatial location of  $u_k$ ,  $v_k^n$  and  $v_k^N$  respectively. Formally,  $\text{enc}(d_k, s)[n, :, :, : 2]$  is a tensor of all negative ones except for  $\text{enc}(d_k, s)[n, \lfloor \frac{s \cdot h}{H} \rfloor, \lfloor \frac{s \cdot w}{W} \rfloor, : 2] = (\frac{s \cdot h}{H} - \lfloor \frac{s \cdot h}{H} \rfloor, \frac{s \cdot w}{W} - \lfloor \frac{s \cdot w}{W} \rfloor)$  where  $u_k = (h, w) \in \Omega = \{1, \dots, H\} \times \{1, \dots, W\}$ . The other 4 channels are defined similarly with  $u_k$  replaced by  $v_k^n$  and  $v_k^N$ .

## B Additional Details of Data Curation

We use the categorization provided by [75] and exclude the 3D models classified as ‘Poor-Quality’ as a pre-filtering step prior to our proposed filtering pipelines (Section 4).

When using GPT-4V to filter Objaverse-Animation into Objaverse-Animation-HQ, we design the following prompt to cover a wide range of cases to be excluded:

**System:** You are a 3D artist, and now you are being shown some animation videos depicting an animated 3D asset. You are asked to filter out some animations. You should filter out the animations that:  
1) have trivial or no motion, i.e., the object is simply scaling, rotating, or moving as a whole without part-level dynamics;  
or 2) depict a scene and only a small component in the scene is moving;  
or 3) have motion that is imaginary, i.e., the motion is not the usual way of how the object moves and it’s hard for humans to anticipate;  
or 4) have very large global motion so that the object exits the frame partially or fully in one of the frames;  
or 5) have changes in object color that are not due to lighting changes;  
or 6) have motion that causes different parts of the same object to disconnect, overlap in an unnatural way, or disappear;  
or 7) have motion that is very chaotic, for example objects exploding or bursting apart.  
**User:** For the following animation (as frames of a video), frame1, frame2, frame3, frame4, tell me, in a single word ‘Yes’ or ‘No’, whether the video should be filtered out or not.

The cost of GPT-4V data filtering is estimated to be \$500.

## C Additional Experiment Details

**Data.** Our final model is fine-tuned on the combined dataset of Drag-a-Move [4] and Objaverse-Animation-HQ (Section 4). During training, we balance over various types of part-level dynamics to control the data distribution. We achieve this by leveraging the categorization provided by [75] and sampling individual data points with the following hand-crafted distribution:  $p(\text{Drag-a-Move}) = 0.3$ ,  $p(\text{Objaverse-Animation-HQ, category ‘Human-Shape’}) = 0.25$ ,  $p(\text{Objaverse-Animation-HQ, category ‘Animals’}) = 0.25$ ,  $p(\text{Objaverse-Animation-HQ, category ‘Daily-Used’}) = 0.05$ ,  $p(\text{Objaverse-Animation-HQ, other categories}) = 0.15$ .

**Architecture.** We zero-initialize the final convolutional layer of each adaptive normalization module before fine-tuning. With our introduced modules, the parameter count is pumped to 1.68B from the original 1.5B SVD.

**Training.** We fine-tune the base SVD on videos of  $256 \times 256$  resolution and  $N = 14$  frames with batch size 64 for 12, 500 iterations. We adopt SVD’s continuous-time noise scheduler, shifting the noise distribution towards more noise with  $\log \sigma \sim \mathcal{N}(0.7, 1.6^2)$ , where  $\sigma$  is the continuous noise level following the presentation in [20]. The training takes roughly 10 days on a single Nvidia A6000 GPU where we accumulate gradient for 64 steps. We enable classifier-free guidance (CFG) [73] by



randomly dropping the conditional drags  $\mathcal{D}$  with a probability of 0.1 during training. Additionally, we track an exponential moving average of the weights at a decay rate of 0.9999.

**Inference.** Unless stated otherwise, the samples are generated using  $S = 50$  diffusion steps. We adopt the linearly increasing CFG [20] with maximum guidance weight 5.0. Generating a single video roughly takes 20 seconds on an Nvidia A6000 GPU.

**Baselines.** For DragNUWA [9] and DragAnything [16], we use their publicly available checkpoints. They operate on a different aspect ratio (*i.e.*,  $576 \times 320$ ). Following previous work [4], we first pad the square input image  $y$  along the horizontal axis to the correct aspect ratio 1.8 and resize it to  $576 \times 320$ , and then remove the padding of the generated frames and resize them back to  $256 \times 256$ . We train DragAPart [4] for 100k iterations using its official implementation on the same combined dataset of Drag-a-Move and Objaverse-Animation-HQ which we used for training Puppet-Master. Since DragAPart is an image-to-image model, we independently generate  $N$  frames conditioned on gradually extending drags to obtain the video. All metrics are computed on  $256 \times 256$  videos.